Thermal equation of state and thermodynamic properties of molybdenum at high pressures

Cite as: J. Appl. Phys. **113**, 093507 (2013); https://doi.org/10.1063/1.4794127
Submitted: 14 December 2012 . Accepted: 19 February 2013 . Published Online: 05 March 2013

Konstantin D. Litasov, Peter I. Dorogokupets, Eiji Ohtani, Yingwei Fei, Anton Shatskiy, Igor S. Sharygin, Pavel N. Gavryushkin, Sergey V. Rashchenko, Yury V. Seryotkin, Yiji Higo, Kenichi Funakoshi, Artem D. Chanyshev, and Sergey S. Lobanov

Thermal equation of state and thermodynamic properties of molybdenum at high pressures

Konstantin D. Litasov,[1,2] Peter I. Dorogokupets,[3] Eiji Ohtani,[4] Yingwei Fei,[5] Anton Shatskiy,[1,2,4] Igor S. Sharygin,[1,2] Pavel N. Gavryushkin,[1,2] Sergey V. Rashchenko,[1,2] Yury V. Seryotkin,[1,2] Yiji Higo,[6] Kenichi Funakoshi,[6] Artem D. Chanyshev,[1,2] and Sergey S. Lobanov[2,5]

[1]*Department of Geology and Geophysics, Novosibirsk State University, Novosibirsk 630090, Russia*
[2]*V.S. Sobolev Institute of Geology and Mineralogy, SB RAS, Novosibirsk 630090, Russia*
[3]*Institute of the Earth's Crust, SB RAS, Irkutsk 664033, Russia*
[4]*Department of Earth and Planetary Materials Science, Graduate School of Science, Tohoku University, Sendai 980-8578, Japan*
[5]*Geophysical Laboratory, Carnegie Institution of Washington, Washington, DC 20015, USA*
[6]*Spring-8, Japan Synchrotron Radiation Research Institute, Kouto, Hyogo 678-5198, Japan*

(Received 14 December 2012; accepted 19 February 2013; published online 5 March 2013)

A comprehensive *P-V-T* dataset for bcc-Mo was obtained at pressures up to 31 GPa and temperatures from 300 to 1673 K using MgO and Au pressure calibrants. The thermodynamic analysis of these data was performed using high-temperature Birch-Murnaghan (HTBM) equations of state (EOS), Mie-Grüneisen-Debye (MGD) relation combined with the room-temperature Vinet EOS, and newly proposed Kunc-Einstein (KE) approach. The analysis of room-temperature compression data with the Vinet EOS yields $V_0 = 31.14 \pm 0.02$ Å^3, $K_T = 260 \pm 1$ GPa, and $K'_T = 4.21 \pm 0.05$. The derived thermoelastic parameters for the HTBM include $(\partial K_T/\partial T)_P = -0.019 \pm 0.001$ GPa/K and thermal expansion $\alpha = a_0 + a_1 T$ with $a_0 = 1.55\ (\pm 0.05) \times 10^{-5}$ K^{-1} and $a_1 = 0.68\ (\pm 0.07) \times 10^{-8}$ K^{-2}. Fitting to the MGD relation yields $\gamma_0 = 2.03 \pm 0.02$ and $q = 0.24 \pm 0.02$ with the Debye temperature (θ_0) fixed at 455-470 K. Two models are proposed for the KE EOS. The model 1 (Mo-1) is the best fit to our *P-V-T* data, whereas the second model (Mo-2) is derived by including the shock compression and other experimental measurements. Nevertheless, both models provide similar thermoelastic parameters. Parameters used on Mo-1 include two Einstein temperatures $\Theta_{E10} = 366$ K and $\Theta_{E20} = 208$ K; Grüneisen parameter at ambient condition $\gamma_0 = 1.64$ and infinite compression $\gamma_\infty = 0.358$ with $\beta = 0.323$; and additional fitting parameters $m = 0.195$, $e_0 = 0.9 \times 10^{-6}$ K^{-1}, and $g = 5.6$. Fixed parameters include $k = 2$ in Kunc EOS, $m_{E1} = m_{E2} = 1.5$ in expression for Einstein temperature, and $a_0 = 0$ (an intrinsic anharmonicity parameter). These parameters are the best representation of the experimental data for Mo and can be used for variety of thermodynamic calculations for Mo and Mo-containing systems including phase diagrams, chemical reactions, and electronic structure. © *2013 American Institute of Physics*. [http://dx.doi.org/10.1063/1.4794127]

I. INTRODUCTION

Accurate determination of the thermodynamic properties and high-temperature equations of state (EOS) for metals is extremely important for condensed matter physics in terms of electronic structure calculations and development of consistent high-pressure scales. Although high-pressure EOS for metals has been extensively studied to extreme conditions both experimentally up to 200–250 GPa (Refs. 1–3) and theoretically up to 10 Mbar and beyond,[4–6] the thermoelastic EOS of most metals and ceramics need to be further refined with new data under simultaneous high pressure and temperature conditions.

Molybdenum (Mo) is a body-centered-cubic (bcc) 4*d* transition metal (structured in *Im*3*m*) with wide engineering and technology applications for its thermal and mechanical strength and chemical resistance. It is also widely used as a pressure standard in diamond anvil cell and shock wave experiments at high pressure.[7–9] Furthermore, a precise EOS is necessary for the calculations of melting curve and phase diagrams. It is also important for developing of buffering techniques for high-pressure experiments because the Mo-MoO_2 buffer is among the most stable at high-temperatures relative to the Fe-FeO oxygen buffer.[10] Thus, the knowledge of the *P-V-T* EOS of Mo is critical for various theoretical and practical applications.

The available data on Mo EOS are from static compression experiments,[2,3,11,12] shock compression experiments,[8,13–20] ultrasonic measurements at high temperature or at high pressure,[21–27] theoretical calculations,[3,28–31] and thermodynamic analysis of experimental data.[28,29,32–35] The only systematic experimental study of *P-V-T* EOS of Mo was performed by Zhao *et al.*[36] in a limited pressure and temperature range up to 10 GPa and 1475 K, restricted by the capacity of technique used. Here, we present new *P-V-T* data for Molybdenum up to 31 GPa and 1673 K and a comprehensive thermal EOS supported by extensive thermodynamic analysis and data reduction from available data.

II. EXPERIMENTAL METHODS

The *in situ* X-ray diffraction experiments were conducted at the SPring-8 synchrotron radiation facility (Japan), using a Kawai-type multi-anvil apparatuses, "SPEED-MkII,"[37] and

"SPEED-1500"[38] installed at a bending magnet beam line BL04B1. An energy-dispersive X-ray diffraction technique was used for the *in situ* measurements. The incident X-rays were collimated to form a thin beam with dimensions of 0.05 mm in the horizontal direction and 0.1 mm in the vertical direction by WC slits and directed to the sample through boron-epoxy window in a pyrophyllite gasket. A Ge solid-state detector with a 4096-channel analyzer was used. The analyzer was calibrated by using characteristic X rays of Cu, Mo, Ag, La, Ta, Pt, Au, and Pb. The diffraction angle (2θ) was ca. 5.5°, calibrated before compression using the known *d*-values of X-ray diffraction peaks of Au (note volumes used in the beam line software: $V_0 = 67.847$ Å^3) or MgO ($V_0 = 71.778$ Å^3), with an uncertainty of less than 0.0005°. In "SPEED-MkII," we used an oscillation system to obtain better X-ray powder diffraction patterns at high temperature by oscillating the press from −3° to 6°. A detailed description of the press system and performance of the oscillation is given by Katsura *et al.*[37]

For experiments (runs #1–2), we used ultra-hard 26 mm WC anvils ("Fuji Die," TF-05) with a truncated edge length (TEL) of 2.0 mm. The sample assembly is nearly the same as that reported by Litasov *et al.*,[39,40] consisting of a Co-doped MgO pressure medium, a cylindrical $LaCrO_3$ heater, molybdenum electrodes, and graphite sample capsule. Low-pressure (<8 GPa) experiments were performed with soft WC anvils (N-05) with a TEL of 12 mm. The cell assemblies included ZrO_2 pressure medium with MgO-insert (for X-ray transparency) and graphite heater. The graphite heater was separated from the graphite sample capsule by a thin BN sleeve. Temperature was monitored by a $W_{97\%}Re_{3\%}$-$W_{75\%}Re_{25\%}$ thermocouple with a junction located at nearly the same position as where the X rays pass through the sample, minimizing the effect on temperature measurements because of the thermal gradient across the sample chamber. The effect of pressure on the thermocouple electromotive forces (emf) was ignored during the experiment.

We used fine-grained Mo powder (99.99%, Rare Metallic) as the starting material. In the run #1, a pressure marker composed of a fine mixture of Au and MgO (1:15) was placed symmetrically to the Mo sample in relation to the temperature field of the cell. The sample and Au-MgO pressure marker were separated by a thin graphite plate. In the runs #2–3 we investigated Mo and W together, which were separated by an MgO plate served as a pressure marker. In the runs #4–5 we investigated 6 starting materials, including Mo, placed in graphite capsule and adjusted with Au or MgO pressure marker (Table I).

In the run #1, the cell assembly was first compressed to nearly the maximum press load at ambient temperature. Thereafter, we followed a complex *PT*-path with several heating cycles (Fig. 1, Table I) while continuously taking diffraction patterns. In the other runs, we performed compression with 1 or 2 heating cycles. Exposure times for collecting diffraction data were 200–400 s. The experimental pressures at high temperature were calculated from the unit cell volume of MgO and/or Au using the EOS presented in this work (Table I). This pressure scale (see below) is similar to that reported in Ref. 41 with <0.05 GPa deviation for Au and <0.3 GPa deviation for MgO at 30 GPa and high temperatures. Typically, 4–5 of the diffraction lines (111), (200), (220), (311), and (222) of Au or MgO were used to calculate the pressures, and 4–5 major diffraction lines were used to calculate the volume of Mo (Fig. 2). We refined X-ray diffraction patterns to determine the *d*-values using the "XRayAnalysis" software provided by the beam line. The uncertainties in the unit cell volume of Au and MgO, determined by a least-squares fit method, give typically less than 0.1 GPa uncertainty in pressure.

The quality of the diffraction patterns and the deviation from hydrostatic conditions during experiment can usually be determined using full width at half maximum (FWHM) of X-ray diffraction lines. The FWHM of X-diffraction lines of Mo, MgO, and Au at the maximum pressure and high temperature was below 10 keV, identical to those at 0.0001–3.0 GPa after heating, indicating that the differential stress is nearly relaxed by high-temperature annealing at all pressures. The precision of the experiments is confirmed by the consistent results obtained using various cell configurations in different runs. We note that an experiment with loading of mixed Mo and MoO_2 was failed presumably due to oxygen dissolution into Mo, which causes significant non-systematic increase of the measured unit cell volume.

The thermal expansion of Mo was also measured at ambient pressure by X-ray diffraction using Thermo Scientific ARL X'TRA diffractometer (Cu$K\alpha$ radiation) equipped with Anton Paar HTK-2000 high-temperature chamber. The sample consisting of Mo powder mixed with CaF_2 internal standard in order to control thermocouple reading[42] was placed on a flat platinum heater. The high-temperature chamber was evacuated down to 10^{-5} bar during the experiment. The results of these measurements will be reported elsewhere. Here, we incorporated the fitted data (Table I) to our thermal equation of state.

The starting material and the recovered samples were also examined with an electron microprobe (JEOL Superprobe JXA-8800) at Tohoku University. An acceleration voltage of 15 kV and 10 nA specimen current were used for the analyses. There were no detectable changes in composition of Mo before and after the experiments. We also did not find signs of carbide formation by reaction with graphite/diamond sample capsule.

III. EQUATIONS OF STATE

We used two conventional approaches to calculate the thermoelastic parameters for Mo, (a) a high-temperature Birch-Murnaghan (HTBM) EOS and (b) a Mie-Grüneisen-Debye (MGD) EOS. The formalism for these approaches can be found in literature.[43–46] Note that using the Vinet/Rydberg EOS for the 298 K isotherm[47] (see discussion in Refs. 48 and 49 for privilege of this EOS) we can obtain similar results with BM EOS at pressures below 1 Mbar while significant deviations may occur at higher pressure. In addition, we performed a comprehensive analysis of EOS and thermodynamic properties of Mo based on the formalism proposed by Dorogokupets *et al.*[35,41,50,51] We named this approach as a Kunc-Einstein (KE) EOS.

TABLE I. Experimental conditions and unit cell volumes of Molybdenum obtained by *in situ* X-ray diffraction. The 1 bar parameters were calculated from measurements by conventional X-ray diffraction. Volumes are in Å^3, pressures are in GPa.

T (K)	V_{Au}	P_{Au}	V_{MgO}	P_{MgO}	V_{Mo}	T (K)	V_{Au}	P_{Au}	V_{MgO}	P_{MgO}	V_{Mo}
Run #1						Run #2					
300	67.85(1)	0	74.71(2)	0	31.146(3)	873	60.52(3)	30.32	65.65(6)	30.44	28.495(3)
300	67.84(1)	0.02	74.71(3)	0.01	31.144(3)	1073	60.79(2)	30.27	65.94(2)	30.50	28.592(3)
300	67.65(1)	0.51	74.40(2)	0.69	31.079(2)	1273	61.10(4)	30.04	66.35(4)	30.13	28.710(3)
300	67.20(2)	1.66	73.92(2)	1.76	30.950(2)	1473	61.48(6)	29.58	66.77(2)	29.78	28.871(3)
300	66.35(1)	4.00	73.01(4)	3.88	30.680(2)	1673	61.85(6)	29.22	67.19(2)	29.47	28.997(3)
300	65.90(2)	5.31	72.39(2)	5.41	30.534(2)	Run #3					
300	65.16(4)	7.62	71.59(2)	7.51	30.323(2)	873			68.26(3)	20.78	29.317(2)
300	63.58(3)	13.16	69.60(4)	13.19	29.752(2)	1073			68.59(3)	20.92	29.399(2)
300	63.53(5)	13.34	69.59(2)	13.23	29.749(2)	1273			69.00(2)	20.83	29.512(2)
300	62.44(2)	17.69	68.12(5)	18.00	29.332(2)	1473			69.64(1)	20.09	29.691(2)
300	61.03(1)	24.08	66.48(3)	23.95	28.826(3)	1673			70.28(1)	19.42	29.917(2)
300	59.62(3)	31.42	64.63(7)	31.56	28.249(3)	1473			69.98(1)	19.06	29.818(2)
473	61.24(2)	24.19	66.67(3)	24.08	28.892(3)	1273			69.94(1)	17.94	29.797(2)
473	62.61(3)	18.12	68.38(3)	18.02	29.387(2)	1073			69.60(3)	17.72	29.706(2)
473	63.78(2)	13.54	69.78(3)	13.55	29.810(2)	873			69.28(2)	17.47	29.639(2)
473	65.43(3)	7.94	71.83(2)	7.78	30.358(2)	673			69.09(2)	16.85	29.592(2)
473	66.72(3)	4.17	73.26(3)	4.21	30.750(2)	473			68.79(1)	16.66	29.529(2)
673	61.54(3)	24.10	66.90(2)	24.39	28.951(3)	300			68.68(1)	16.13	29.512(2)
673	62.88(3)	18.32	68.59(4)	18.47	29.437(2)	Run #4					
673	64.07(2)	13.81	70.09(4)	13.80	29.863(2)	873	66.35(2)	7.94			30.530(2)
673	65.78(1)	8.21	72.14(2)	8.16	30.422(2)	1073	66.84(2)	7.98			30.655(2)
673	67.08(3)	4.58	73.54(2)	4.75	30.790(2)	1273	67.40(1)	7.93			30.813(2)
873	61.74(3)	24.50	67.14(3)	24.69	28.972(2)	1473	68.00(2)	7.89			30.964(2)
873	63.14(2)	18.63	68.88(2)	18.74	29.496(2)	1673	68.67(2)	7.80			31.122(2)
873	64.35(2)	14.18	70.32(2)	14.34	29.908(2)	1073	67.54(2)	6.20			30.852(2)
873	66.15(4)	8.52	72.47(2)	8.55	30.476(2)	873	67.21(2)	5.63			30.761(2)
873	67.44(2)	5.05	73.86(2)	5.26	30.853(2)	673	66.87(2)	5.14			30.740(2)
873	68.28(3)	3.04	74.92(2)	2.94	31.095(2)	473	66.58(1)	4.54			30.712(2)
1073	61.98(3)	24.72	67.43(3)	24.88	29.057(3)	300	66.28(1)	4.20			30.651(2)
1073	63.40(2)	18.97	69.15(2)	19.12	29.562(3)	Run #5					
1073	63.17(4)	19.83	68.87(3)	20.01	29.478(3)	300			74.71(2)	0	31.158(2)
1073	64.63(3)	14.57	70.61(2)	14.75	29.981(2)	1273			77.23(2)	1.01	31.647(2)
1073	66.42(3)	9.11	72.75(2)	9.11	30.536(2)	1073			76.53(2)	1.03	31.515(2)
1073	67.74(3)	5.71	74.23(2)	5.68	30.909(2)	873			75.92(3)	0.93	31.384(2)
1073	68.89(2)	3.12	75.45(4)	3.12	31.217(2)	673			75.30(3)	0.92	31.244(2)
1273	61.50(3)	28.19	66.85(4)	28.24	28.880(3)	473			74.83(3)	0.70	31.176(2)
1273	62.12(4)	25.46	67.60(4)	25.52	29.103(3)	300			74.11(2)	1.32	30.982(2)
1273	63.35(4)	20.46	69.11(3)	20.47	29.560(3)	473			74.50(2)	1.40	31.067(2)
1273	63.61(2)	19.48	69.38(2)	19.63	29.656(2)	673			75.01(3)	1.52	31.175(2)
1273	64.80(2)	15.36	70.74(2)	15.62	30.046(2)	1473			77.10(2)	2.50	31.618(2)
1273	66.71(4)	9.70	73.06(2)	9.62	30.615(2)	1273			76.48(2)	2.38	31.472(2)
1273	68.15(2)	6.15	74.51(2)	6.33	31.012(2)	1073			75.81(2)	2.40	31.317(2)
1273	69.64(4)	3.02	76.02(3)	3.25	31.379(2)	873			75.03(2)	2.72	31.132(2)
1473	61.94(4)	27.54	67.35(4)	27.67	29.030(2)	673			74.40(1)	2.82	31.011(2)
1473	62.34(3)	25.81	67.85(4)	25.89	29.173(2)	473			74.43(2)	1.56	31.047(2)
1473	63.61(3)	20.81	69.38(2)	20.87	29.637(2)	300			74.07(2)	1.41	30.982(2)
1473	65.01(4)	16.02	71.02(3)	16.09	30.089(2)	300			74.71(2)	0.01	31.150(2)
1473	66.87(1)	10.67	73.14(2)	10.67	30.642(2)	1 bar					
1673	62.36(5)	27.03	67.84(2)	27.17	29.171(3)	300					31.141(5)
1673	64.11(4)	20.36	69.88(2)	20.59	29.800(3)	473					31.243(5)
Run #2						673					31.367(5)
300	67.85(2)	0	74.71(2)	0	31.145(3)	873					31.499(5)
300	59.69(9)	31.03	64.71(9)	31.21	28.280(4)	1073					31.639(5)
473	59.93(6)	30.84	64.86(7)	31.40	28.349(4)	1273					31.786(5)
673	60.16(6)	30.87	65.17(4)	31.23	28.397(3)	1473					31.942(5)

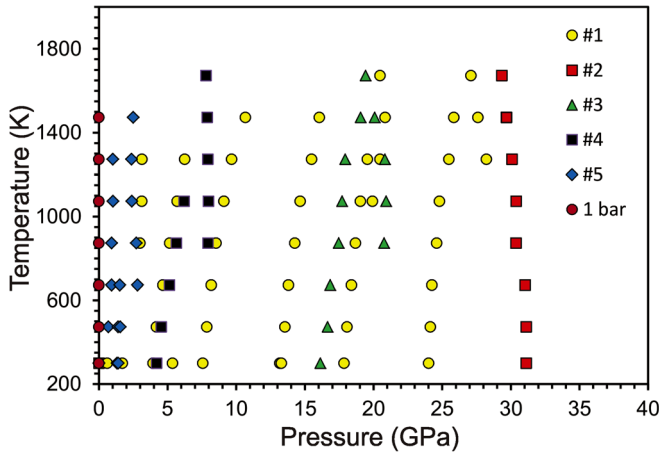

FIG. 1. Pressure-temperature paths of *in situ* X-ray diffraction experiments. The pressures were calculated using MgO EOS. 1 *bar* shows results of experiment at the ambient conditions.

A. High-temperature Birch-Murnaghan EOS

We follow Litasov *et al.*[52,53] in abbreviations and symbols. The third-order Birch-Murnaghan EOS is given by the following expression:

$$P = 1.5\,K_T(z^{7/3} - z^{5/3}) \times [1 + 0.75(K_T' - 4)(z^{2/3} - 1)], \tag{1}$$

where K_T is a isothermal bulk modulus, $z = V_{0T}/V$, V_{0T} volume at 1 atm, V high-pressure volume, and K_T' pressure derivative of K_T. The temperature effect on K_T and V_{0T} is expressed as follows:

$$K_T = K_{T0} + (\partial K_T/\partial T)_P(T - T_0), \tag{2}$$

$$V_{0T} = V_0 \exp\left[\int_{T_0}^{T} \alpha dT\right], \tag{3}$$

where $(\partial K_T/\partial T)_P$ is a temperature derivative of the bulk modulus, T_0 reference temperature (298.15 K), and α volumetric thermal expansion at atmospheric pressure. The thermal expansion α is expressed as $\alpha(T) = a_0 + a_1 T$. K_T' is assumed to be a constant with temperature. In this approach we optimize six parameters V_0, K_{T0}, K_T', $(\partial K_T/\partial T)_P$, a_0, and a_1, by fitting the *P-V-T* data to the HTBM EOS.

B. Mie-Grüneisen-Debye EOS

The MGD formalism includes following expression for the thermal pressure ΔP_{th} in addition to static pressure at 300 K from the Vinet EOS:

$$\mathrm{D}P_{th} = \gamma/V[E_{th}(V,T) - E_{th}(V,T_0)], \tag{4}$$

where γ is the Grüneisen parameter and E_{th} is thermal energy. The thermal energy is calculated from the Debye model as follows:

$$E_{th} = \frac{9nRT}{(\theta/T)^3}\int_0^{\theta/T} \frac{\xi^3}{e^{\xi} - 1} d\xi, \tag{5}$$

where n is number of atoms in a formula unit, R the gas constant, and θ the Debye temperature. The volume dependence of θ and γ is described by following equations:

$$\theta = \theta_0 \exp[(\gamma_0 - \gamma)/q], \tag{6}$$

$$\gamma = \gamma_0(V/V_0)^q, \tag{7}$$

where q is dimensionless parameter. In this approach, the six fitted parameters are V_0, K_{T0}, K_T', γ_0, θ_0, and q.

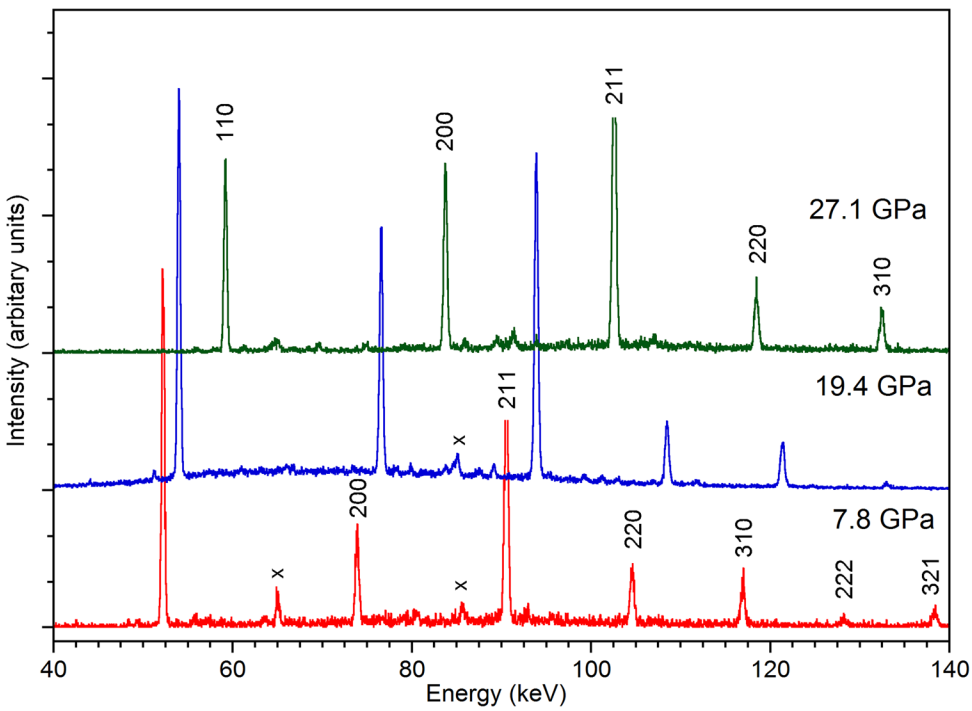

FIG. 2. Representative X-ray diffraction patterns of Mo collected at 1673 K and different pressures. Unidentified peaks are marked by x.

C. Kunc-Einstein EOS

In contrast to the MGD EOS this approach approximates high-pressure static *P-V-T* data along with thermochemical, ultrasonic, and shock compression data via the Helmholtz free energy expression[54–56]

$$F = U_0 + E_0(V) + F_{th}(V,T) - F_{th}(V,T_0) + F_e(V,T) - F_e(V,T_0) + F_{anh}(V,T) - F_{anh}(V,T_0), \quad (8)$$

where U_0 is the reference energy; $E_0(V)$ is the potential (cold) part of the free energy at the reference isotherm, corresponding to T_0 (298.15 K), which depends only on V; $F_{th}(V,T)$ is the thermal part of the free energy, which depends on V and T; $F_e(V,T)$ and $F_{anh}(V,T)$ are the terms, describing electronic contribution and intrinsic anharmonicity, which also depend on V and T. Differentiation of Eq. (8) allows calculations of entropy (S), internal energy (E), isochoric heat capacity (c_V), pressure (P), isothermal bulk modulus (K_T), pressure slope at constant volume ($(\partial P/\partial T)_V = \alpha K_T$), thermal expansion ($\alpha$), enthalpy ($H$), and Gibbs free energy (G).[41,50]

Analysis of different EOS for 298 K isotherm shows universality of the EOS proposed by Kunc *et al.*[57]

$$P(V) = 3K_T y^{-k}(1-y)\exp[\eta(1-y)], \quad (9)$$

where $y = (V/V_0)^{1/3}$, $\eta = 3K_T'/2 - k + 1/2$, and k is an additional parameter, which can be fitted. Equation (9) can be transformed to the Vinet/Rydberg EOS or to the Holzapfel EOS.[58] For metals we obtained best results using $k = 2$ (Vinet/Rydberg), and for silicates, with $k = 5$ (Holzapfel).

The thermal part of Helmholtz free energy can be written via Einstein model with two characteristic temperatures Θ_1 and Θ_2, which depend on V

$$F_{th}(V,T) = m_1 \mathrm{R}T \ln\left(1 - \exp\frac{-\Theta_1}{T}\right) + m_2 \mathrm{R}T \ln\left(1 - \exp\frac{-\Theta_2}{T}\right) - \frac{3}{2} n\mathrm{R}e_0 x^g T^2 - \frac{3}{2} n\mathrm{R}a_0 x^m T^2. \quad (10)$$

Here $x = V/V_0$, $m_1 + m_2 = 3n$, e_0 denotes an electronic contribution to the free energy, a_0 is an intrinsic anharmonicity parameter, which can be equal to zero, m is an anharmonicity equivanent of the Grüneisen parameter, and g is an electronic equivalent of the Grüneisen parameter. This approach provides consistency of the calculated standard entropy with its reference values. For simplification, we consider equations for a single characteristic temperature. Differentiating Eq. (10) at constant volume, one can obtain expression for the entropy and the thermal energy

$$S = -\left(\frac{\partial F}{\partial T}\right)_V = 3n\mathrm{R}\left[-\ln\left(1 - \exp\frac{-\Theta}{T}\right) + \frac{\Theta/T}{\exp(\Theta/T) - 1}\right] + 3n\mathrm{R}e_0 x^g T + 3n\mathrm{R}a_0 x^m T, \quad (11)$$

$$E_{th} = F_{th} + TS = 3n\mathrm{R}\left[\frac{\Theta}{\exp(\Theta/T) - 1}\right] + \frac{3}{2} n\mathrm{R}e_0 x^g T^2 + \frac{3}{2} n\mathrm{R}a_0 x^m T^2. \quad (12)$$

In turn, differentiating Eq. (10) at constant temperature we can reveal the thermal pressure

$$P_{th} = -\left(\frac{\partial F_{th}}{\partial V}\right)_T = 3n\mathrm{R}\frac{\gamma}{V}\left[\frac{\Theta}{\exp(\Theta/T) - 1}\right] + \frac{3}{2} n\mathrm{R}e_0 x^g T^2 \frac{g}{V} + \frac{3}{2} n\mathrm{R}a_0 x^m T^2 \frac{m}{V}. \quad (13)$$

Differentiating Eq. (12) at constant volume and Eq. (13) at constant temperature, we can express the isochoric heat capacity $C_V = (\partial E/\partial T)_V$ and the isothermal bulk modulus $K_T = -V(\partial P/\partial V)_T$ as follows:

$$C_V = 3n\mathrm{R}\left[\left(\frac{\Theta}{T}\right)^2 \frac{\exp(\Theta/T)}{[\exp(\Theta/T) - 1]^2}\right] + 3n\mathrm{R}e_0 x^g T + 3n\mathrm{R}a_0 x^m T, \quad (14)$$

$$K_T = 3n\mathrm{R}\frac{\gamma}{V}\left[\frac{\Theta}{\exp(\Theta/T) - 1}\right] \times (1 + \gamma - q) + \frac{3}{2} n\mathrm{R}e_0 x^g T^2 \frac{g}{V}(1-g) + \frac{3}{2} n\mathrm{R}a_0 x^m T^2 \frac{m}{V}(1-m). \quad (15)$$

Differentiating Eq. (13) at constant volume obtains the pressure slope as

$$(\partial P/\partial T)_V = \gamma/VC_V. \quad (16)$$

Finally, we can calculate other thermodynamic parameters of interest, including the coefficient of thermal expansion, $\alpha = (\partial P/\partial T)_V/K_T$, the isobaric heat capacity, $C_P = C_V + \alpha^2 TVK_T$, and the adiabatic bulk modulus $K_S = K_T + VT(\alpha K_T)^2/C_V$, which can be compared with values obtained by direct measurements using different types of experiments. The enthalpy and Gibbs free energy can be calculated from $H = E + PV$ and $G = F + PV$.

As shown in Eqs. (13), (15), and (16), two new parameters were appeared upon differentiation, which are the Grüneisen parameter, $\gamma = -(\partial \ln \Theta/\partial \ln V)_T$ and parameter $q = (\partial \ln \gamma/\partial \ln V)_T$. We expressed their volume dependence via the form of Al'tshuler *et al.*:[59] $\gamma = \gamma_\infty + (\gamma_0 - \gamma_\infty)\, x^\beta$, where γ_0 is the Grüneisen parameter at standard conditions, γ_∞ is the Gruneisen parameter at infinite compression ($x = 0$), and β is a fitted parameter, which is related to q in the MGD expression for γ.

The volume dependence of the characteristic temperature and parameter q are calculated from

$$\Theta = \Theta_0 x^{-\gamma_\infty} \exp\left[\frac{\gamma_0 - \gamma_\infty}{\beta}(1 - x^\beta)\right], \quad (17)$$

TABLE II. Thermoelastic parameters for Mo obtained using HTBM EOS.

Parameter	1	2	3	4	5	6
V_{0T}, Å^3	31.140 (5)	31.14[a]	31.15	31.15	31.16(1)	31.19 (4)
K_{T0}, GPa	268 (2)	260[a]	266 (9)	268 (1)	255 (1)	262 (2)
K_T'	3.94 (9)	4.21[a]	4.1 (9)	3.81 (6)	4.08 (1)	4.05 (1)
a_0, 10^{-5} K^{-1}	1.266 (61)	1.547 (57)	1.32 (14)	1.31 (10)	1.56 (3)	1.50 (5)
a_1, 10^{-8} K^{-2}	1.014 (71)	0.680 (74)	1.26 (15)	1.12 (11)	0.23 (2)	0.10 (1)
$(\partial K_T/\partial T)_P$, GPa K^{-1}	−0.0243 (12)	−0.0193 (9)	−0.034 (9)	−0.021 (3)	−0.0163 (2)	−0.0124 (6)

[a]Fixed according to optimized parameters (see text). 1 and 2, experimental data, this work; 3 and 4, experimental data and those reduced with shock Hugoniot;[36] 5, thermodynamic approximation;[35] 6, theoretical EOS.[31]

$$q = \beta x^{\beta} \frac{\gamma_0 - \gamma_\infty}{\gamma}. \quad (18)$$

The assumption that $\gamma_\infty = 0$ leads to the usual MGD form $\gamma = \gamma_0 x^{\beta}$, where β is equal to q.

In addition, we can combine the described formalism using KE EOS with shock Hugoniot data. The details of these calculations can be found elsewhere.[35] Thus, we determined all thermodynamic parameters, which are necessary to constrain KE EOS for the particular material. The procedure for finding the thermodynamic parameters for EOS was described previously.[50] Some of the input parameters can be assumed based on the other experimental data, similar to obtaining V_0 and K_T—from static or shock compression experiments. Parameters $m_1 = m_2 = 1.5$ allow correct description of C_P at temperatures from 100 K. Initial value for γ_0 can be derived from independent measurements and the initial γ_∞ can be fixed at 0.66.[60,61]

Other parameters are entirely fitted and can be obtained by simultaneously weighted least-squares fitting of the available high-pressure *P-V* and *P-V-T* data, experimental data on the heat capacity, thermal expansion, and adiabatic bulk modulus at zero pressure and various temperatures. The full solution allowed us to find all the necessary parameters for KE EOS, which include V_0, K_{T0}, K_T', Θ_{E10}, Θ_{E20}, m_{E1}, m_{E2}, γ_0, γ_∞, β, e_0, a_0, m, and g. With the described formalism we can then calculate any thermodynamic functions versus T and V or versus T and P.

IV. RESULTS AND DISCUSSION

The reported unit cell volume of Mo at 298.15 K and 1 bar varies from 31.12 to 31.17 Å^3 (Refs. 2, 3, and 62). Our experimentally determined value is $V_0 = 31.145 \pm 0.005$ Å^3, averaged from several measurements at ambient conditions. Table I lists the unit cell parameters of Mo measured in the present experiments up to 31.6 GPa and 1673 K along with pressures calculated using MgO and Au pressure markers. Representative X-ray diffraction patterns of Mo at high *P-T* conditions are shown in Fig. 2. The results of the fitting of *P-V-T* data using different approaches are presented in Tables II–IV and plotted in Fig. 3.

Pressures were calibrated using the Au and MgO pressure scales calculated using similar KE EOS approach with the parameters listed in Table IV. As mentioned before, the calculated pressures are consistent with those reported by Dorogokupets and Dewaele[41] within the uncertainties. All three approaches used for the calculations of EOS in this study provide consistent results, and the differences can be seen only by extrapolation of our data beyond 1–2 Mbar and at high temperatures (Fig. 4). The MGD fitting is possible only with fixed Debye temperature, using reference data,[22,26,36] because the fitting of experimental *P-V-T* data yields unrealistically high Debye temperature (Table III). The pressures calculated using KE EOS for Mo are compared with those calculated from calibrants used in different studies in Fig. 5. Low-pressure data (<35 GPa) show that experimental conditions have some small influence on the calculated volumes and pressures for Mo. For example, the run #3 overestimates pressures for 0–0.5 GPa, whereas

TABLE III. Thermoelastic parameters for Mo obtained using MGD EOS.

Parameter	1	2	3	4	5
V_{0T}, Å^3	31.147 (6)	31.14[a]	31.14[a]	31.28(2)	31.14[a]
K_{T0}, GPa	268 (2)	260[a]	249 (1)	239 (1)	245 (1)
K_T'	3.94 (9)	4.21[a]	4.47 (5)	4.70 (1)	4.66 (1)
γ_0	2.42 (5)	2.03 (2)	1.98 (1)	1.82 (4)	1.97 (2)
q	0.90 (29)	0.24 (2)	1.99 (4)	0.69 (5)	0.82 (3)
θ_0, K	1370 (80)	455–470[a]	470[a]	366 (110)	470[a]

[a]Fixed according to optimized parameters (see text). Debye temperature is fixed according to reference data.[22,26,36] 1 and 2, this work; 3, Ref. 35; 4 and 5, theoretical EOS.[31]

TABLE IV. Parameters of Mo obtained using KE EOS. Mo-1: based on present *P-V-T* data, static compression, and thermochemical data; Au, MgO and Mo-2: based on thermodynamic analysis including shock compression data (modified to present formalism from Refs. 35 and 65).

Parameters	Au	MgO	Mo-1	Mo-2
V_0, cm^3/mol	10.215	11.248	9.376	9.376
K_{T0}, GPa	167.0	160.3	260	260.0
K_T'	5.90	4.25	4.21	4.21
k	2	5	2	2
Θ_{E10}, K	178.7	747	366	414
$m_{E1} = m_{E2}$	1.5	3	1.5	1.5
Θ_{E20}, K	83.3	399	208	191
γ_0	2.940	1.530	1.644	1.64
γ_∞	1.71	0.624	0.358	3.20
β	5.06	2.115	0.323	0.51
$a_0 \times 10^6$, K^{-1}	–9.4	–15.9	0	62
M	7.55	4.48	0.195	3.26
$e_0 \times 10^6$, K^{-1}	6.1	0	90	74.1
g	0.66	0	5.6	2.256

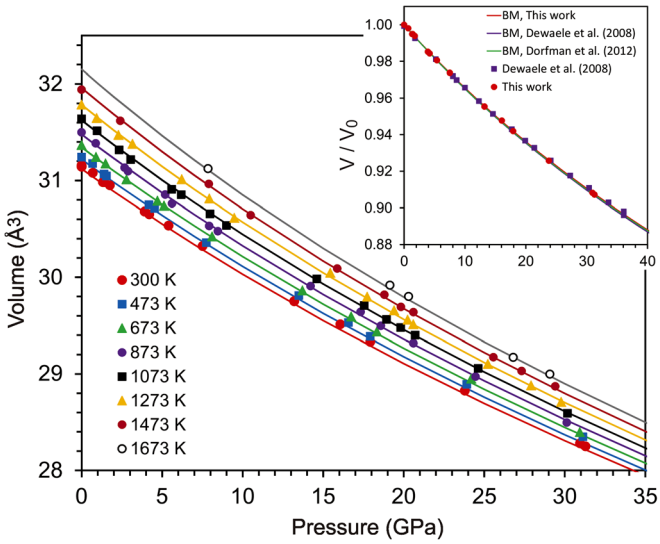

FIG. 3. KE EOS fit to *P-V-T* data for Mo. Solid lines are isothermal compression curves at 300, 473, 673, 873, 973, 1073, 1273, 1473, and 1673 K. Insert shows compressibility curves at room temperature fitted by BM EOS. The data points and fitted curves are indistinguishable from reference data[2,3] in the studied pressure range.

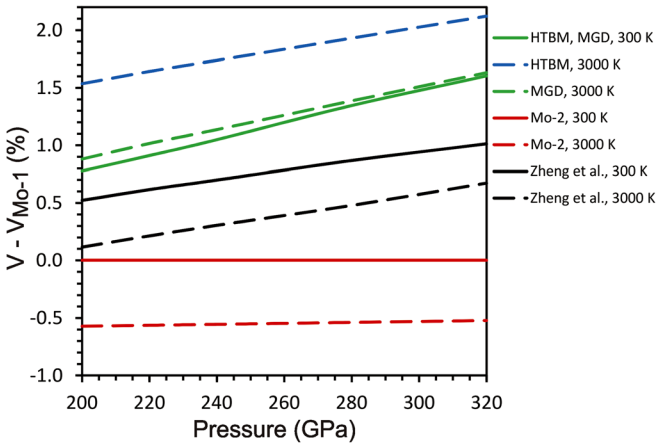

FIG. 4. Comparison of different EOS in this work using parameters listed in Tables II–IV with theoretical EOS.[31] The calculated volumes along 300 and 3000 K isotherms are related to model Mo-1.

the runs# 4–5 may slightly underestimate pressures. The pressures calculated for the data by Zhao *et al.*[36] obtained using the NaCl pressure scale show slightly overestimation in pressure, but within −0.1 to +0.7 GPa (Fig. 5(a)). High pressure static compression data were found in good agreement with our KE EOS for Mo. Data from Dewaele *et al.*[3] slightly overestimate pressures, whereas data from Dorfman *et al.*[2] show underestimation for 0–2 GPa, still within 3% uncertainty (Fig. 5(b)).

Sometimes single experiment is enough to obtain consistent *P-V-T* data for a material at high pressure using multianvil apparatus. However, in case of Mo we obtained high thermal expansion coefficient in run #1 relative to previous data at 1 bar. We should note that Zhao *et al.*[36] obtained even higher thermal expansion coefficient in their experiments (Table II, Fig. 6).

In order to clarify this inconsistency, we performed additional experiments with single or double heating circles at pressures below 2 GPa. The data obtained in these experiments (runs #2–5) were found in an excellent agreement with the data from run #1 (Figs. 3 and 5). We further measured volume expansion of Mo at 1 bar using X-ray diffraction in high-vacuum camera at 298–1473 K and obtained results that are consistent with the results of our high-pressure experiments (Fig. 3). It is not clear, what is the cause for some inconsistency between our data and previous measurements of the thermal expansion (Fig. 6), but we have obtained consistent results from several different measurements.

We have developed two models (Mo-1 and Mo-2), which are both calculated using KE EOS but based on slightly different approaches: Mo-1 using the measured *P-V-T* data as the primary data and Mo-2 also including the reduced shock compression data (Table IV). The model Mo-1 strictly corresponds to present *P-V-T* data set and the model Mo-2 is more consistent with all thermodynamic parameters determined at ambient conditions and shock compression data. Nevertheless,

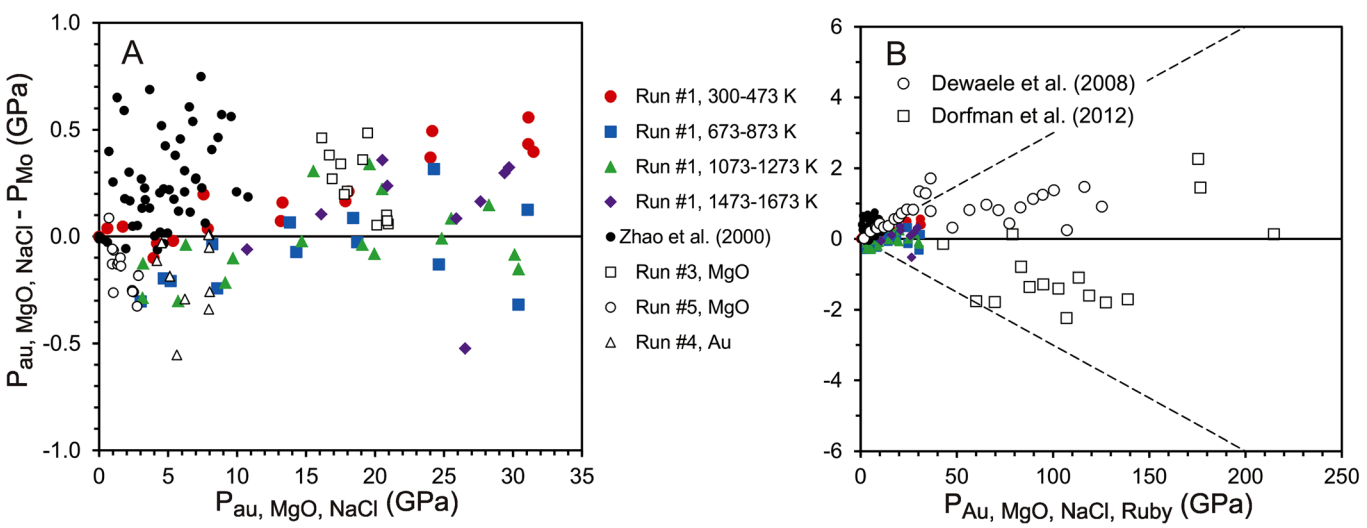

FIG. 5. Differences between pressures calculated using EOS of pressure standards used in previous works[2,3,36] and pressures calculated using KE EOS of Mo (model Mo-1). (a) Moderate pressures, (b) high pressures. The dotted lines show 3% deviation from the zero value. The data from Dewaele *et al.*[3] are recalculated by Ruby scale[35,65] and those from Dorfman *et al.*[2] are recalculated using MgO scale from Table IV.

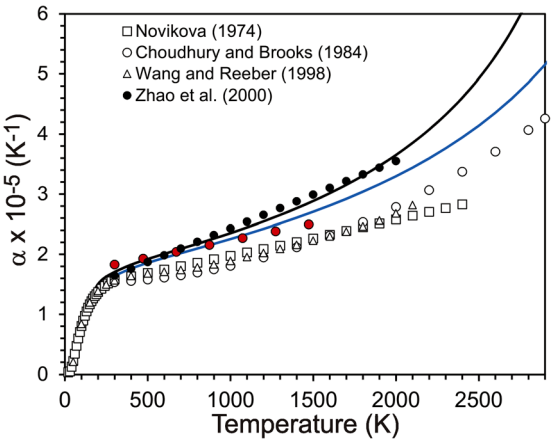

FIG. 6. Calculated thermal expansion coefficient of Mo in comparison in with reference data.[64,66,67] Black lines—values calculated using Mo-1 model, blue lines—calculated using Mo-2 model. Red circles represent fit of diffraction data at ambient conditions (this work).

the differences between these two models are only 0.5% uncertainty in V_{Mo} at 320 GPa and 3000 K (Fig. 4). Calculated thermodynamic parameters for Mo-1 are shown in Tables V and VI.

Both Mo-1 and Mo-2 show perfect consistency with experimental heat capacity data for C_P (Fig. 7). Indeed, the calculated entropy ($S_{0,298} = 28.55$ J/(mol K) in Mo-1 and $S_{0,298} = 28.73$ J/(mol K) in Mo-2) is consistent with the reference data $S_{0,298} = 28.6$ J/(mol K).[63]

The $K_T = 268$ GPa and $K'_T = 3.94$ calculated from the simple HTBM and MGD approaches are in reasonable agreement with data obtained from static compression, ultrasonic measurements, and shock compression experiments, $K_T = 260$ GPa and $K'_T = 4.21$.[3,35] In the pressure range of this study (up to 31 GPa), the 300 K isothermal curves are indistinguishable from both sets of parameters because of the trade-off between K_T and K'_T (Fig. 3). In order to perform consistent analysis to derive the thermal parameters, we fixed $K_T = 260$ GPa and $K'_T = 4.21$ along with V_0 (Tables II). We obtained K_T as a function of temperature by fitting to the *P-V-T* data in this study using the simple HTBM approach. The result is in a good agreement with other experimental

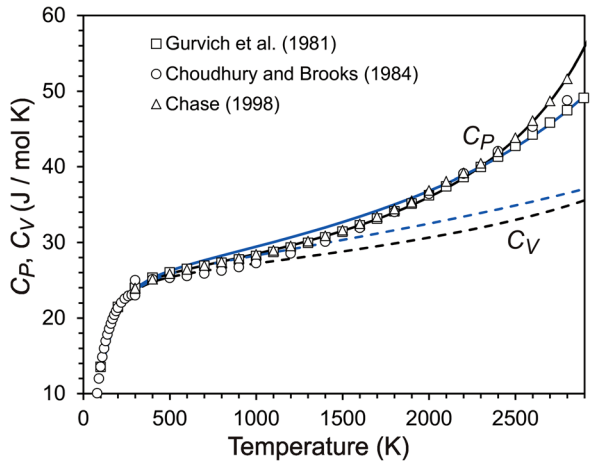

FIG. 7. Comparison of calculated heat capacities of Mo with reference data for C_P.[63,64,68] Black lines—values calculated using Mo-1 model, blue lines—calculated using Mo-2 model.

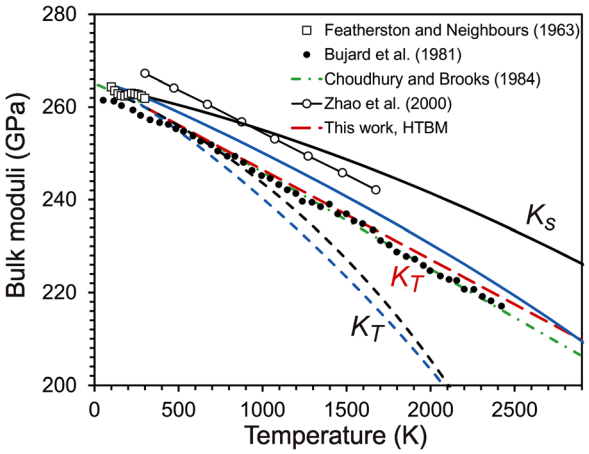

FIG. 8. Calculated bulk moduli of Mo in comparison with reference data for K_S.[22,27] The data for K_S obtained by Choudhury and Brooks[64] coincide with those by Miller *et al.*[13] Black lines—values calculated using Mo-1 model, blue lines—calculated using Mo-2 model.

data (Fig. 8). The calculated K_S from the Mo-1 is not perfectly consistent with experimental measurements[22,27] and analytical curves,[13,64] whereas Mo-2 gives more consistent results.

Previous estimations of the thermal Grüneisen parameters range from $\gamma_0 = 1.52$ (Ref. 13) to 1.75 (Ref. 36). In this study, we obtained $\gamma_0 = 1.64$ in Altshuler form using KE and $\gamma_0 = 1.8$–2.0 using MGD form. The values derived from the model Mo-1 seem too high, whereas the model Mo-2 yielded consistent results with shock wave data[18] and theoretical calculations[31] (Fig. 9).

Several equations of state of Mo have been proposed in the previous studies. We noticed clear consistency in the 298 K isotherm with the previous data from static compression experiments (Fig. 3).[2,3] The data by Zhao *et al.*[36] for limited pressure range up to 10 GPa provided useful results (slightly overestimating thermal expansion), but with no doubt have high uncertainty when they are extrapolated to higher pressures. We can compare our data with the thermal EOS of Mo calculated from *ab initio* simulations.[31] Indeed, we provided appropriate verification for theoretical EOS. The EOS of Zeng *et al.*[31] has some clear differences in the calculated thermodynamic parameters. For example, the

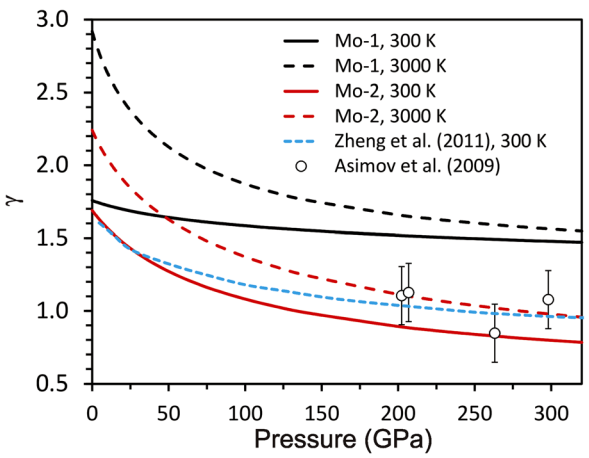

FIG. 9. Variations of Grüneisen parameter with *P* at different *T*. Data from shock compression experiments[18] and theoretical curve[31] are shown.

TABLE V. Calculated thermodynamic parameters for Mo at different pressures and temperatures using KE EOS (Mo-1 model in Table IV).

P	T	$y=V/V_0$	$\alpha\times10^{-5}$	S	C_P	C_V	K_T	K_S	γ	ΔG
(Gpa)	(K)		(K^{-1})		(J mol^{-1} K^{-1})		(GPa)	(GPa)		(KJ mol^{-1})
0.0001	298.15	1.0000	1.70	28.55	23.88	23.66	260.0	262.3	1.756	0
0.0001	500	1.0037	1.92	41.43	25.82	25.38	256.0	260.5	1.824	−7.157
0.0001	1000	1.0145	2.35	60.17	28.48	27.20	243.6	255.1	2.003	−33.019
0.0001	1500	1.0278	2.89	72.27	31.53	28.79	227.1	248.7	2.193	−66.282
0.0001	2000	1.0445	3.65	81.90	36.00	30.63	205.4	241.4	2.399	−104.885
0.0001	2500	1.0669	4.92	90.67	43.67	32.98	176.2	233.3	2.632	−148.039
0.0001	3000	1.0998	7.68	99.89	60.87	36.40	134.2	224.3	2.918	−195.623
100	298.15	0.7890	0.73	19.69	21.31	21.23	620.6	622.7	1.583	820.828
100	500	0.7903	0.83	31.47	23.91	23.75	617.6	621.7	1.601	815.585
100	1000	0.7938	0.92	48.67	25.56	25.18	609.7	618.9	1.651	795.104
100	1500	0.7975	0.97	59.19	26.36	25.72	600.8	615.7	1.703	767.976
100	2000	0.8016	1.03	66.88	27.10	26.15	590.8	612.3	1.757	736.376
100	2500	0.8058	1.10	73.01	27.88	26.56	579.7	608.6	1.812	701.355
100	3000	0.8104	1.17	78.17	28.75	26.98	567.4	604.6	1.870	663.530
200	298.15	0.6926	0.49	15.56	19.61	19.57	929.2	931.2	1.518	1511.405
200	500	0.6934	0.58	26.69	23.02	22.91	926.4	930.5	1.526	1507.073
200	1000	0.6955	0.64	43.41	24.91	24.67	919.3	928.4	1.550	1489.121
200	1500	0.6978	0.66	53.64	25.54	25.14	911.7	926.0	1.576	1464.697
200	2000	0.7001	0.69	61.05	25.97	25.41	903.6	923.5	1.602	1435.942
200	2500	0.7026	0.71	66.89	26.37	25.63	895.0	920.9	1.630	1403.908
200	3000	0.7051	0.73	71.73	26.77	25.83	885.9	918.1	1.658	1369.221
300	298.15	0.6306	0.37	12.91	18.19	18.16	1214.9	1216.9	1.478	2129.984
300	500	0.6312	0.46	23.50	22.29	22.22	1212.2	1216.3	1.482	2126.252
300	1000	0.6327	0.51	39.88	24.56	24.37	1205.4	1214.6	1.497	2110.001
300	1500	0.6344	0.53	49.97	25.17	24.87	1198.3	1212.6	1.512	2087.380
300	2000	0.6361	0.54	57.26	25.53	25.11	1191.0	1210.6	1.528	2060.491
300	2500	0.6378	0.55	62.99	25.82	25.28	1183.3	1208.5	1.544	2030.378
300	3000	0.6396	0.56	67.72	26.08	25.41	1175.3	1206.3	1.561	1997.668

calculated V_0 for bcc-Mo is 32.06 Å^3, which is almost 3% higher than the measured value. This difference is common for the *ab initio* computations. At ambient conditions, this difference in volume corresponds to a temperature change of 1500 K. There are also clear differences in the calculated entropy ($S_{0,298}=41$ J/mol K) and thermal expansion (Table II). However, the differences in the absolute values of V_{Mo} at 200–300 GPa between the calculations and the model Mo-1 become smaller (less than 1%).

TABLE VI. Relative volumes (V/V_0) of *bcc*-Mo as a function of pressure and temperature using KE EOS (Mo-1 model in Table IV). $V_0=31.14$ Å^3.

	T (K)						
P (GPa)	298.15	500	1000	1500	2000	2500	3000
0.0001	1.0000	1.0037	1.0145	1.0278	1.0445	1.0669	1.0998
5	0.9817	0.9850	0.9947	1.0064	1.0208	1.0392	1.0641
10	0.9649	0.9680	0.9768	0.9873	0.9999	1.0155	1.0356
20	0.9353	0.9379	0.9454	0.9541	0.9642	0.9762	0.9907
30	0.9096	0.9119	0.9184	0.9258	0.9343	0.9440	0.9554
40	0.8870	0.8890	0.8948	0.9013	0.9085	0.9167	0.9261
50	0.8667	0.8686	0.8737	0.8795	0.8859	0.8930	0.9010
100	0.7890	0.7903	0.7938	0.7975	0.8016	0.8058	0.8104
150	0.7344	0.7354	0.7380	0.7409	0.7438	0.7469	0.7502
200	0.6926	0.6934	0.6955	0.6978	0.7001	0.7026	0.7051
250	0.6588	0.6595	0.6613	0.6632	0.6651	0.6672	0.6692

V. SUMMARY

In summary, we have obtained a comprehensive *P-V-T* dataset for bcc-Mo at pressures from 0.0001 to 31 GPa and temperatures up to 1673 K using MgO and Au pressure calibrants. The thermodynamic analysis of these data was performed using HTBM EOS and MGD approaches combined with the room-temperature Vinet EOS, and newly proposed KE approach. In the HTBM and MGD approaches, only the *P-V-T* data were used in the fitting, without constraints from other independently derived thermodynamic parameters. In the KE approach, we established a self-consistent thermodynamic model where all the parameters were accounted for. As a result, we can calculate free energy for the wide range of pressures and temperatures. It also allows reliable calibration of Mo EOS to the pressures of at least 300 GPa and temperatures up to 4000 K.

A detailed analysis of room-temperature compression curve with Vinet EOS provides $V_0=31.14\pm0.02$ Å^3, $K_T=260\pm1$ GPa, and $K_T'=4.21\pm0.05$, which are consistent with previous data. The estimated thermoelastic parameters from HTBM include $(\partial K_T/\partial T)_P=-0.019\pm0.001$ GPa/K and thermal expansion $\alpha=a_0+a_1T$ with $a_0=1.55$ $(\pm0.05)\times10^{-5}$ K^{-1} and $a_1=0.68$ $(\pm0.07)\times10^{-8}$ K^{-2}. The parameters used in the MGD model are $\gamma_0=2.03\pm0.02$ and $q=0.24\pm0.02$ at Debye temperature (θ_0,) fixed at 455–470 K.

We have proposed two KE EOS models by fitting our *P-V-T* data only (Mo-1) and by integration of the available data including shock compression results (Mo-2). Nevertheless, both models yield similar thermoelastic parameters. In Mo-1, the optimized parameters include two Einstein temperatures $\Theta_{E1o} = 366$ K, $\Theta_{E2o} = 208$ K, Grüneisen parameter at ambient condition $\gamma_0 = 1.64$ and infinite compression $\gamma_\infty = 0.358$ with $\beta = 0.323$, and additional fitting parameters $m = 0.195$, $e_0 = 0.9 \times 10^{-6}$ K^{-1}, and $g = 5.6$. The fixed parameters include $k = 2$ in Kunc EOS, $m_{E1} = m_{E2} = 1.5$ in expression for Einstein temperature, and $a_0 = 0$.

The calculations of *P-V-T* data and thermodynamic parameters for Mo and other metals and species are available online via http://labpet.crust.irk.ru. Excel spreadsheet for the Mo EOS calculations is available by the request from the authors.

ACKNOWLEDGMENTS

We thank the reviewers for critical comments and suggestions. This work was conducted as a part of the Global Center-of-Excellence Program "Global Education and Research Center for Earth and Planetary dynamics" at Tohoku University and supported by the Ministry of education and science of Russia, Project 14.B37.21.0457, Integration project of Siberian Branch RAS No. 97 for 2012-2014, and Russian Foundation for Basic Research (No. 12-05-00758-a). Experiments were conducted under SPring-8 general research proposal Nos. 2009A1278, 2009B1327, and 2012B1289.

[1]A. Dewaele, P. Loubeyre, and M. Mezouar, Phys. Rev. B **70**, 094112 (2004).
[2]S. M. Dorfman, V. B. Prakapenka, Y. Meng, and T. S. Duffy, J. Geophys. Res., [Solid Earth] **117**, B08210 (2012).
[3]A. Dewaele, M. Torrent, P. Loubeyre, and M. Mezouar, Phys. Rev. B **78**, 104102 (2008).
[4]D. Batani *et al*., Phys. Rev. Lett. **88**, 235502 (2002).
[5]A. L. Ruoff, C. O. Rodriguez, and N. E. Christensen, Phys. Rev. B **58**, 2998 (1998).
[6]D. Alfe, G. D. Price, and M. J. Gillan, Phys. Rev. B **64**, 045123 (2001).
[7]H. K. Mao, P. M. Bell, J. W. Shaner, and D. J. Steinberg, J. Appl. Phys. **49**, 3276 (1978).
[8]S. P. Marsh, *LASL Shock Hugoniot Data* (University of California Press, Berkeley, 1980).
[9]C. E. Ragan III, M. G. Silbert, and B. C. Diven, J. Appl. Phys. **48**, 2860 (1977).
[10]H. S. C. O'Neill, Am. Mineral. **71**, 1007 (1986).
[11]L. C. Ming and M. H. Manghnani, J. Appl. Phys. **49**, 208 (1978).
[12]Y. K. Vohra and A. L. Ruoff, Phys. Rev. B **42**, 8651 (1990).
[13]G. H. Miller, T. J. Ahrens, and E. M. Stolper, J. Appl. Phys. **63**, 4469 (1988).
[14]R. S. Hixson, D. A. Boness, J. W. Shaner, and J. A. Moriarty, Phys. Rev. Lett. **62**, 637 (1989).
[15]A. C. Mitchell, W. J. Nellis, J. A. Moriarty, R. A. Heinle, N. C. Holmes, R. E. Tipton, and G. W. Repp, J. Appl. Phys. **69**, 2981 (1991).
[16]R. S. Hixson and J. N. Fritz, J. Appl. Phys. **71**, 1721 (1992).
[17]R. F. Trunin, M. A. Podurets, G. V. Simakov, L. V. Popov, and A. G. Sevast'yanov, High Temp. **32**, 736 (1994).
[18]P. D. Asimow, D. Y. Sun, and T. J. Ahrens, Phys. Earth Planet. Inter. **174**, 302 (2009).
[19]K. K. Krupnikov, A. A. Bakanova, M. I. Brazhnik, and R. F. Trunin, Dokl. Akad. Nauk SSSR **148**, 1302 (1963).
[20]A. M. Molodets, High Press. Res. **25**, 211 (2005).
[21]D. I. Bolef and J. De Klerk, J. Appl. Phys. **33**, 2311 (1962).
[22]F. H. Featherston and J. R. Neighbours, Phys. Rev. **130**, 1324 (1963).
[23]J. M. Dickinson and P. E. Armstrong, J. Appl. Phys. **38**, 602 (1967).
[24]D. L. Davidson and F. R. Brotzen, J. Appl. Phys. **39**, 5768 (1968).
[25]K. W. Katahara, M. H. Manghnani, and E. S. Fisher, J. Phys. F **9**, 773 (1979).
[26]W. Liu, Q. Liu, M. L. Whitaker, Y. Zhao, and B. Li, J. Appl. Phys. **106**, 043506 (2009).
[27]P. Bujard, R. Sanjines, E. Walker, J. Ashkenazi, and M. Peter, J. Phys. F **11**, 775 (1981).
[28]B. K. Godwal and R. Jeanloz, Phys. Rev. B **41**, 7440 (1990).
[29]J. A. Moriarty, Phys. Rev. B **45**, 2004 (1992).
[30]A. B. Belonoshko, S. I. Simak, A. E. Kochetov, B. Johansson, L. Burakovsky, and D. L. Preston, Phys. Rev. Lett. **92**, 195701 (2004).
[31]Z.-Y. Zeng, C.-E. Hu, X.-R. Chen, X.-L. Zhang, L.-C. Cai, and F.-Q. Jing, Phys. Chem. Chem. Phys. **13**, 1669 (2011).
[32]Y. Wang, D. Q. Chen, and X. W. Zhang, Phys. Rev. Lett. **84**, 3220 (2000).
[33]Z. Tian, L. Wang, R. Xiong, and J. Shi, J. Mater. Sci. **44**, 708 (2009).
[34]A. Karbasi, S. K. Saxena, and R. Hrubiak, CALPHAD: Comput. Coupling Phase Diagrams Thermochem. **35**, 72 (2011).
[35]T. S. Sokolova, P. I. Dorogokupets, and K. D. Litasov, Russ. Geol. Geophys. **54**, 181 (2013).
[36]Y. S. Zhao, A. C. Lawson, J. Z. Zhang, B. I. Bennett, and R. B. Von Dreele, Phys. Rev. B **62**, 8766 (2000).
[37]T. Katsura, K. Funakoshi, A. Kubo, N. Nishiyama, Y. Tange, Y. Sueda, T. Kubo, and W. Utsumi, Phys. Earth Planet. Inter. **143–144**, 497 (2004).
[38]W. Utsumi, K. Funakoshi, S. Urakawa, M. Yamakata, K. Tsiji, H. Konishi, and O. Shimomura, Rev. High Pressure Sci. Technol. **7**, 1484 (1998).
[39]K. Litasov, E. Ohtani, A. Sano, A. Suzuki, and K. Funakoshi, Earth Planet. Sci. Lett. **238**, 311 (2005).
[40]K. D. Litasov, E. Ohtani, Y. Nishihara, A. Suzuki, and K. Funakoshi, J. Geophys. Res., [Solid Earth] **113**, B08205 (2008).
[41]P. I. Dorogokupets and A. Dewaele, High Press. Res. **27**, 431 (2007).
[42]B. Schumann and H. Neumann, Cryst. Res. Technol. **19**, K13 (1984).
[43]O. L. Anderson, *Equations of State of Solids for Geophysics and Ceramic Science* (Oxford University Press, Oxford, 1995).
[44]F. Birch, J. Geophys. Res. **57**, 227, doi:10.1029/JZ057i002p00227 (1952).
[45]I. Jackson and S. M. Rigden, Phys. Earth Planet. Inter. **96**, 85 (1996).
[46]J. P. Poirier, *Introduction to the Physics of the Earth's Interior*, 2nd ed. (Cambridge University Press, Cambridge, UK, 2000).
[47]P. Vinet, J. Ferrante, J. H. Rose, and J. R. Smith, J. Geophys. Res. **92**, 9319, doi:10.1029/JB092iB09p09319 (1987).
[48]S. Gaurav, B. S. Sharma, S. B. Sharma, and S. C. Upadhyaya, Physica B **322**, 328 (2002).
[49]F. D. Stacey, B. J. Brennan, and R. D. Irvine, Geophys. Surv. **4**, 189 (1981).
[50]P. I. Dorogokupets and A. R. Oganov, Phys. Rev. B **75**, 024115 (2007).
[51]P. I. Dorogokupets, Phys. Chem. Miner. **37**, 677 (2010).
[52]K. D. Litasov, E. Ohtani, S. Ghosh, Y. Nishihara, A. Suzuki, and K. Funakoshi, Phys. Earth Planet. Inter. **164**, 142 (2007).
[53]K. D. Litasov, A. Shatskiy, Y. W. Fei, A. Suzuki, E. Ohtani, and K. Funakoshi, J. Appl. Phys. **108**, 053513 (2010).
[54]V. N. Zharkov and V. A. Kalinin, *Equations of State of Solids at High Pressures and Temperatures* (Consultants Bureau, New York, 1971).
[55]J. Ita and L. Stixrude, J. Geophys. Res., [Solid Earth] **97**, 6849 (1992).
[56]W. B. Holzapfel, Z. Kristallogr. **216**, 473 (2001).
[57]K. Kunc, I. Loa, and K. Syassen, Phys. Rev. B **68**, 094107 (2003).
[58]W. B. Holzapfel, Rep. Prog. Phys. **59**, 29 (1996).
[59]L. V. Al'tshuler, S. E. Brusnikin, and E. A. Kuz'menkov, J. Appl. Mech. Tech. Phys. **28**, 129 (1987).
[60]A. M. Molodets, D. V. Shakhray, A. A. Golyshev, L. V. Babare, and V. V. Avdonin, High Press. Res. **26**, 223 (2006).
[61]W. B. Holzapfel, M. Hartwig, and W. Sievers, J. Phys. Chem. Ref. Data **30**, 515 (2001).
[62]M. E. Straumanis and R. P. Shodhan, Trans. Metall. Soc. AIME **242**, 1185 (1968).
[63]M. W. Chase, J. Phys. Chem. Ref. Data **9**, 1 (1998).
[64]A. Choudhury and C. R. Brooks, Int. J. Thermophys. **5**, 403 (1984).
[65]P. I. Dorogokupets, T. S. Sokolova, B. S. Danilov, and K. D. Litasov, Geodyn. Tectonophys. **3**, 129 (2012).
[66]K. Wang and R. R. Reeber, Mater. Sci. Eng. R. **23**, 101 (1998).
[67]S. I. Novikova, *Thermal Expansion of Solids* (Nauka, Moscow, 1974).
[68]L. V. Gurvich, I. V. Veits, and V. A. Medvedev, *Thermodynamic Properties of Individual Substances* (Nauka, Moscow, 1981).